J Nanopart Res (2011) 13:1175–1182
DOI 10.1007/s11051-010-0109-x

RESEARCH PAPER

The synthesis of Ag/polypyrrole coaxial nanocables via ion adsorption method using different oxidants

Teng Qiu · Huxiao Xie · Jiangru Zhang · Amad Zahoor · Xiaoyu Li

Received: 11 March 2010 / Accepted: 1 October 2010 / Published online: 20 October 2010

Abstract Ag/polypyrrole (PPy) coaxial nanocables (NCs) were synthesized by an ion adsorption method. In this method, the pre-made Ag nanowires (NWs) were dispersed in the aqueous solution of copper acetate ($Cu(Ac)_2$), and the Cu^{2+} ions adsorbed onto the surface of Ag NWs can oxidize pyrrole monomers to polymerize into uniform PPy sheath outside Ag NWs after the $Cu(Ac)_2$-treated Ag NWs were re-dispersed in the aqueous solution of pyrrole. The morphology of NCs was characterized by transmission electron microscope (TEM) and scanning electron microscope (SEM). The relationship between the thickness of polymer sheath and the concentration of $Cu(Ac)_2$ was established. As $Cu(Ac)_2$ which served as the oxidant can also be replaced by $AgNO_3$ in this synthesis, the differences on the structure of polymer sheath caused by different oxidants were studied by surface-enhanced Raman scattering (SERS), high-resolution transmission electron microscope (HR-TEM), Fourier transform infrared spectroscopy (FT-IR), and X-ray photoelectron spectroscopy (XPS). Comparing with the characterization results of Ag/PPy NCs synthesized using $AgNO_3$ as the oxidant which indicates the random arrangement of PPy chains at the interface between polymer sheath and Ag NWs, PPy chain oxidized by Cu^{2+} tends to show a relatively ordered conformation at the interface with the pyrrole rings identically taking the plane vertical to the surface of Ag NWs. In addition, although the main part of the polymer sheath was composed of PPy whatever kind of oxidant was used, the sheath of the NCs oxidized by Cu^{2+} is typical for the existence of Cu(I)–pyrrole coordinate structures with strong Cu(I)–N bond signal shown in XPS characterization.

Keywords Coaxial nanocables · Ion adsorption · Redox · Polypyrrole · Silver nanowires · One-dimensional nanomaterials

T. Qiu · H. Xie · J. Zhang · A. Zahoor · X. Li (✉)
College of Materials Science and Engineering, Key Laboratory of Carbon Fiber and Functional Polymers, Ministry of Education, Beijing University of Chemical Technology, Beijing 100029, People's Republic of China
e-mail: lixy@mail.buct.edu.cn

Introduction

The synthesis of one-dimensional nanomaterials has attracted tremendous attentions in these days (Xia et al. 2003; Tang and Kotov 2005). Among the various nanomaterials with different morphologies such as nanowires (NWs) (Goldberger et al. 2006), nanorods (Park et al. 2007), nanotubes (Kuemmeth et al. 2008), coaxial nanocables (NCs) are one of the most widely concerned architectures (Zhang et al. 2007; Guo et al. 2009). NCs are typical for their cable-like morphology with a core NW coated by a proper uniform sheath (Tian et al. 2007). Believed to be able to improve the carrier collection and overall efficiency with respect to the simple NWs, NCs have

great potential applications in sensors or electric devices (Jang and Bae 2007). Great devotes have been done developing methods to produce coaxial NCs with efficiency. Many kinds of NCs have been successfully prepared in the past decades, and their unique properties incorporated with their special structure design, including the conductive, magnetic, and luminescent capability, have been fairly explored (Wang et al. 2009; Zhang et al. 1998).

A typical example of the omnifarious NCs is Ag/polypyrrole (PPy) NCs (Zhang and Manohar 2005; Zhang et al. 2003). Methods such as layer-by-layer deposition (Mayya et al. 2001), hydro-thermal method (Yu et al. 2004), in situ polymerization (Xu et al. 2005), and one step method (Chen et al. 2005) have been applied in the synthesis of Ag/PPy NCs. The simple mechanism including the function of the tailoring agent poly(vinylpyrrolidone) (PVP) has also been reported (Xiong et al. 2006; Gao et al. 2004). It has been reported by our group that Ag/PPy coaxial NCs can be successfully fabricated at room temperature based on the adsorption of oxidative "common ions" on the surface of Ag NWs followed by a redox polymerization carried out in pyrrole solutions (Chen et al. 2006). The oxidant used in this method is $AgNO_3$. Further work in our groups showed that not only Ag^+, which is so-called "common ions," but other oxidative ions such as Cu^{2+} are also able to be loaded onto the surface of Ag NWs (Xie et al. 2008). Actually $AgNO_3$ is not a very desirable oxidant for the preparation of NCs because of its strong acidity and strong oxidation ability which will have negative effects on the morphologies or the conductivities of the sheath polymers. The replacement of $AgNO_3$ by other oxidant with weaker acidity and weaker oxidation ability is with its advantages.

In this study, Ag/PPy coaxial NCs were prepared by a modified "common ion adsorption method" using copper acetate ($Cu(Ac)_2$) as the oxidant. As the polymerization of pyrrole monomers on Ag NWs was oxidized by Cu^{2+} instead of Ag^+, the methods can be renamed as "ion adsorption method" in this way. Moreover, surface-enhanced Raman scattering (SERS) was applied on the characterization of NCs. The polymer structures, especially the difference on molecule conformation at the interface between Ag and PPy sheath caused by using different oxidants ($AgNO_3$ and $Cu(Ac)_2$), were discussed in detail. No longer restricted by the rules of "common ions," the work here is trying to provide a versatile method for the fabrication of nanometal/polymer composites based on the redox polymerization although further exploration and optimization on the method are still needed. The incorporation of possible different metal ions on the polymer sheath may introduce extraordinary properties which are desirable to the wide potential applications in nanodevices and single molecule detections.

Experimental

The preparation of Ag NWs

Silver NWs were synthesized by polyol reduction using PVP as the tailoring agent (Sun and Xia 2002). In a typical synthesis, 6 mL of 0.1 M $AgNO_3$ and 6 mL of 0.15 M PVP solution in ethylene glycol (EG) were injected simultaneously into a three-neck bottle precharged with 10 mL EG. The reaction was carried out under reflux at 160 °C for 60 min. After the mixture was cooled down to room temperature, it was isolated by centrifugation at 4000 rpm for 30 min. The bottom layer in the centrifuge tube was collected as the coarse product. The coarse product was washed three times by acetone and then by ethanol, separately. In a typical washing procedure, the isolated coarse product was diluted by the solvent (acetone or ethanol, five times of the product in volume). The dilution was dispersed by ultrasonication for 15 min. After that, centrifugation was applied at 4000 rpm for 30 min with the bottom layer in the centrifuge tube collected. The obtained products were finally washed once by deionized water. The thoroughly washed products were immediately dispersed in the aqueous solution of oxidant ($Cu(Ac)_2$ or $AgNO_3$) for further fabrication.

The fabrication of Ag/PPy NCs

The detailed synthesis of Ag/PPy NCs using $AgNO_3$ as the oxidant (NCs–$AgNO_3$) was reported elsewhere (Chen et al. 2006). The synthesis of Ag/PPy NCs using $Cu(Ac)_2$ as the oxidant (NCs–$Cu(Ac)_2$) is similar to that. As-synthesized Ag NWs were dispersed in 20 mL $Cu(Ac)_2$ aqueous solution by ultrasonication for 20 min. The treated NWs were isolated by centrifugation and then redispersed in 20 mL of deionized water containing 0.5 mL of

dissolved pyrrole monomer. The reaction was carried out in a round-bottomed flask at room temperature for 48 h under magnetic stirring. The final products were isolated by centrifugation at 4000 rpm for 30 min with the bottom layer in the centrifuge tube collected as the coarse product. The coarse product was washed thoroughly with the procedure similar with that in the synthesis of Ag NWs, but the solvent was replaced by water and ethanol, separately. After dried in vacuum at 60 °C for 48 h, the final product was obtained as black solid powder which was stored in vacuum.

Characterization

The morphology of NCs was observed by transmission electron microscope (TEM; HITACHI-800) operated at 100 kV and high-resolution transmission electron microscope (HR-TEM; FEI TECNAI F20) operated at 200 kV equipped with an electron diffraction (ED). Scanning electron microscopy (SEM) characterization was carried out on XL-30 ESEM-FEG from FEI. Fourier Transform Infrared (FT-IR) spectra were obtained using Bruker Tensor37. Raman spectra were recorded on a Renishaw System 1000 Raman imaging microscope (Renishaw plc, UK) equipped with a 25 mW (632.8 nm) He–Ne laser and a peltier-cooled CCD detector. The laser was focused onto a spot of approximately 1 μm in diameter by a 50× objective mounted on an Olympus BH-2 microscope. Zeta-potential of Ag NWs and Ag/PPy NCs was measured by Malvern NanoZS using ethanol as the dispersant. X-ray photoelectron spectroscopy (XPS) was obtained using ThermoVG Escalab 250.

Results and discussion

TEM images of Ag NWs and Ag/PPy NCs are shown in Fig. 1. Ag NWs obtained from polyol reduction method were with smooth surfaces and uniform diameters (40–50 nm, Fig. 1, inset). Clear PPy sheath can be observed in the TEM image (Fig. 1, main image) of our final NCs–$Cu(Ac)_2$. The SEM image of Ag/PPy NCs–$Cu(Ac)_2$ is shown in Fig. 2 with Ag NWs entirely coated by scale-like polymers. The thickness of PPy sheath is depended on the concentration of $Cu(Ac)_2$ in aqueous solution ($[Cu(Ac)_2]$) which was used in the treatment of Ag NWs before they were added in the monomer solution. The relationship between the thickness of PPy sheath and the concentration of $Cu(Ac)_2$ aqueous solution is shown in Fig. 3 as the square line. The sheath thickness kept increasing with the increase of $[Cu(Ac)_2]$. When $[Cu(Ac)_2]$ reached 0.35 M, the thickness of PPy sheath could reach 40 nm, almost two times as much as the maximum thickness obtained from NCs–$AgNO_3$ (Xie et al. 2008).

Although the distribution of particle size in our system is broad observed from the TEM results, the nanocomposites, especially the Cu^{2+}-loaded Ag NWs, can be well dispersed in ethanol which permits us to measure the zeta-potential of the NWs with acceptable and repeatable results. The relationship between the zeta-potential of $Cu(Ac)_2$-treated Ag

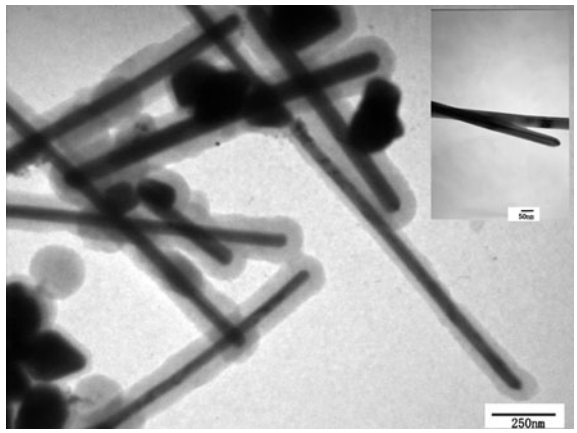

Fig. 1 A typical TEM image of Ag/PPy NCs ($[Cu(Ac)_2]$ = 0.25 M). *Inset* bare silver nanowires

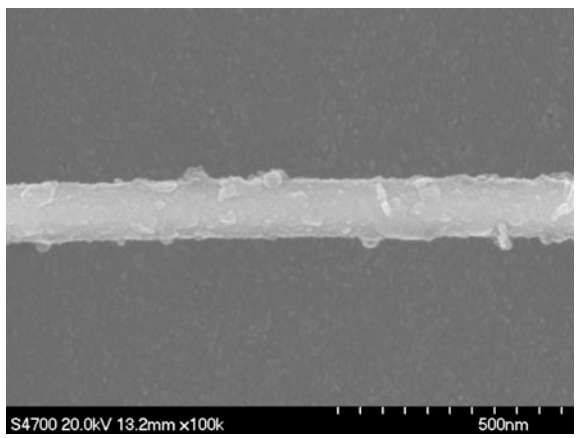

Fig. 2 A typical SEM image of Ag/PPy NCs

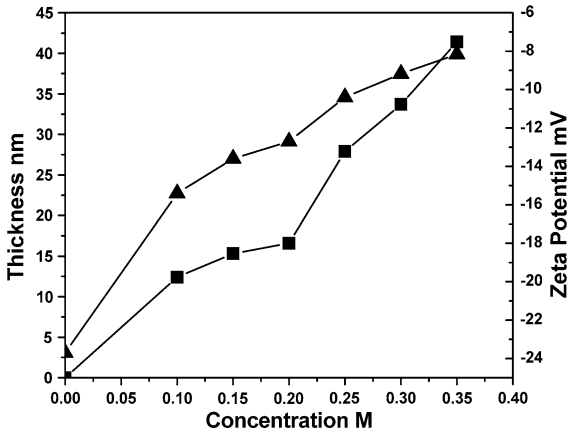

Fig. 3 The relationship between the thickness of PPy sheath and the concentration of $Cu(Ac)_2$ aqueous solution (*square*), and the relationship between the zeta-potential of the silver NWs and the concentration of $Cu(Ac)_2$ aqueous solution (*triangle*)

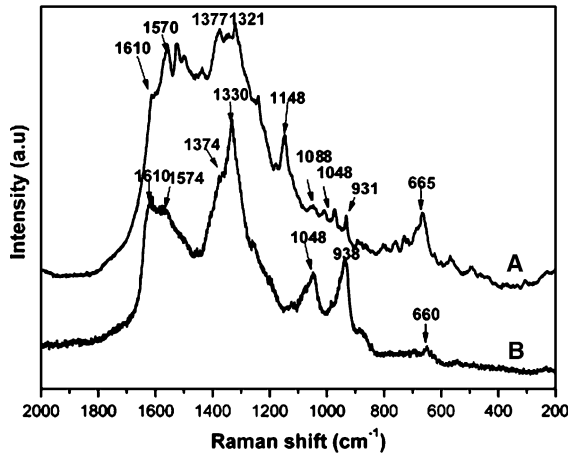

Fig. 4 Raman spectra of Ag/PPy NCs oxidized by (*A*) $AgNO_3$; (*B*) $Cu(Ac)_2$

NWs and $[Cu(Ac)_2]$ is also shown in Fig. 3. For as-prepared Ag NWs ($[Cu(Ac)_2] = 0$), the zeta-potential of NWs is below −24 mV. After Ag NWs were dispersed in $Cu(Ac)_2$ solution, Cu^{2+} ions would adsorb onto the surface of Ag NWs driven by the columbic attraction. The adsorption of positive ions will neutralize part of the negative charges on the surface of NWs, which correspondingly caused the increase on the zeta-potential value in the positive direction. In this way, the increase on the zeta-potential value means the increase on the amount of the compensated Cu^{2+} ions adsorbed on the surface of Ag NWs. With the increase of the concentration of $Cu(Ac)_2$ in aqueous solution, the two curves in Fig. 3 are of similar trends. If we simply attribute the increase on zeta-potential to the increase amount of Cu^{2+} adsorbed on the surface of Ag NWs, we can confer that the more ions of Cu^{2+} adsorbed on Ag NWs, the thicker will the polymer sheath be, i.e., the thickness of the polymer sheath is reliable to the concentration of Cu^{2+} on Ag NWs. The adsorbed Cu^{2+} ions should be served as the active centers to initiate the polymerization of pyrrole monomers for the formation of PPy sheath when $Cu(Ac)_2$-treated Ag NWs were redispersed in pyrrole solution.

One of the characteristic properties of Ag NWs is the SERS effect (Wang and Zhang 2009). The spectrum of SERS is only sensitive to the molecule layer just on the surface of the substrate made by some noble metal which is served by Ag NWs in this study. The characteristic is useful in the characterization of PPy chains at the interface between the PPy sheath and the Ag NWs inside. Raman spectra of the two kinds of Ag/PPy NCs are shown in Fig. 4 with the NCs prepared using $AgNO_3$ (A) and $Cu(Ac)_2$ (B) as the oxidants, respectively. The strong intensities and high resolutions of the spectra indicate the effective enhancing effect on the Raman signals provided by the specialties of the surface of Ag NWs.

It can be found that typical peaks for PPy structures are shown in both of the two spectra (Han et al. 2005). Most of the peaks are of about the same locations in the two spectra with only a little shift which were caused possibly by the operations. However, there are still markable differences between the two spectra. First, in Fig. 4A, there are two remarkable peaks at 1148 and 665 cm^{-1} which are nearly disappeared in Fig. 4B. The peaks at 1148 and 665 cm^{-1} in Fig. 4A are attributed to the out-of-plane deformation mode of the aromatic ring and C–H bond, respectively. In general, the out-of-plane vibration here involves a dipole moment perpendicular to the plane of aromatic rings in the PPy chain. According to "surface selection rules" for SERS (Moskovits and Suh 1984), i.e., only molecule vibrational peaks giving rise to a dynamic dipole moment along the direction perpendicular to the surface of the substrate should be observed in the vibration spectrum, some of the PPy chains must take the conformation with the plane of pyrrole rings flat on the surfaces of Ag NWs so that the enhancement on the two peaks which belong to the

out-of-plane vibration can be illustrated. But in Fig. 4B, the two peaks are almost absent, i.e., the enhanced Raman bands are all attributed to the in-plane vibration, which involves a dipole moment parallel to the plane of the aromatic rings in the molecule. Thus, the pyrrole rings should much more prefer to "stand up" with the plane of pyrrole ring vertical to the surface of NWs rather than to lean or lie on the surface. In this conformation, the out-of-plane vibration gives rise to a dynamic dipole moment parallel to the surface of Ag NWs so that the cancel of the peaks at 1148 and 665 cm^{-1} in Fig. 4B can be illustrated. With all the aromatic rings "standing up" at the surface of Ag NWs, the PPy polymer chains should take an ordered conformation at the interface between Ag NWs and PPy sheath.

Another difference between the two spectra in Fig. 4 is on the peaks belonging to C=C symmetrical stretching vibration. The Raman band for C=C symmetrical stretching vibration can be divided into two peaks located at about 1610 and 1574 cm^{-1}, separately. In Fig. 4A, the intensity of the peak at 1610 cm^{-1} is much lower than that at 1574 cm^{-1}. In Fig. 4B, the relative intensity of the peak at 1610 cm^{-1} is much increased with its intensity a little stronger than the intensity of the peak at 1574 cm^{-1}. Although the increase on the extent of oxidation of PPy might cause the enhancement of the relative intensity of the peak at 1610 cm^{-1}, it does not work in the case because the sample for Fig. 4B is synthesized using $Cu(Ac)_2$ as the oxidant which is a weaker oxidant compared to $AgNO_3$ used in the synthesis of the sample for Fig. 4A. In Fig. 4B, the relatively intensities of the peaks attributing to the neutral state (peaks at 1330 and 1048 cm^{-1}) are much stronger than the peaks attributing to the oxidized states (peaks at 1374 and 1088 cm^{-1}). However, in Fig. 4A, the peaks at 1374 and 1088 cm^{-1} is very strong with their intensities comparable to the intensities of their adjacent peaks for neutral state at 1330 and 1048 cm^{-1}, respectively. Proved by the above comparison on SERS spectra, the extent of oxidation of PPy characterized in Fig. 4B is much lower than that in Fig. 4A. Therefore, the possible reason for the increase on the intensity of the peak at 1610 cm^{-1} can also be attribute to the conformation of PPy chains at the interface between Ag NWs and PPy sheath. If the PPy chains at the interface take an relatively ordered conformation, the rod-like arrangement of the aromatic segment can elongate the conjugation length on polymer chains which gives rise to the enhanced intensity of the peak at 1610 cm^{-1} (Kiani et al. 1992; Chen et al. 2003).

The HR-TEM image and the ED results on the different regions of NCs–$Cu(Ac)_2$ are shown in Fig. 5. The ED pattern of Ag NWs inside (region A) is consistent with the FCC Ag single crystals in bulk. The electronic diffract of the polymer sheath (region C) shows only a diffuse halo, which indicates that the main part of PPy sheath is amorphous. Interestingly, when we tried to focus the electron beam on the interface (region B), both of the diffuse lattice and the diffuse halo are overlapped in the diffuse pattern of region B which results to a complicated pattern. However, the clear interface layer can be distinguished between Ag NWs and PPy sheath with a thickness of about 9 nm (region B) in the photograph of HR-TEM shown left in Fig. 5. The image contrast between the interface layer (region B) and the main part of the PPy sheath (region C) indicates that the polymer conformation here is different from those outside. The special ordered conformation of the polymer chains located at the interface region has been confirmed again. The ordered arrangement came possibly from the template effect of the surface of the Ag NWs. The "standing" conformation of the aromatic rings on the surface of Ag NWs could be stabilized by the coordination of the N atoms on the pyrrole rings and the Ag atoms at the surface of NWs with the delocationalized π electrons. For the case using $AgNO_3$ as the oxidant, the etching of the by-produced H^+ and the deposition of reduced Ag particles would robust the Ag NWs surface, which is benefit for enhancing the Raman signals by SERS effect but unfavorable for the formation of ordered structures. As mentioned previously, Ag^+ ions are stronger oxidant than Cu^{2+} ions, which means an accelerated propagation rate of the polymer chains. The rapid increase on the molecule weight of the polymer makes the molecule hardly have enough time to adjust its conformation to the most preferable position. As a result, the PPy molecules should take a random conformation at the interface between Ag NWs and polymer sheath of Ag NWs–$AgNO_3$. But the effect of the surface template is restricted to the near-surface layer of Ag NWs–$AgNO_3$. As shown in

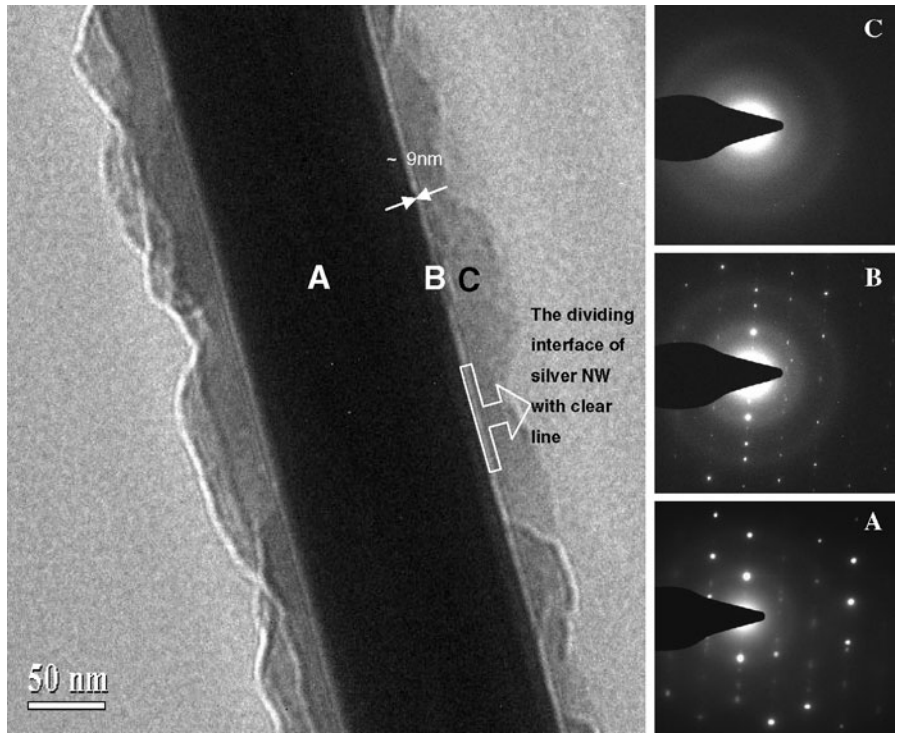

Fig. 5 HR-TEM and ED of Ag/PPy NCs oxidized by $Cu(Ac)_2$

the ED images, the main part of the PPy sheath (part C) is amorphous. This phenomena is similar to the results in Davidson's work in which a PPy film with crystalline structure was prepared by electrochemical methods (Davidson et al. 1996).

FT-IR spectra of Ag/PPy NCs using different oxidants are shown in Fig. 6. The typical peaks for PPy are shown in both spectra, such as the peaks at 3427 cm^{-1} (N–H stretching vibration), 1085 cm^{-1} (C–H deformation mode), 1560 cm^{-1} (ring stretching vibration), which confirms the PPy structure in sheath. However, in Fig. 6B which is for NCs–$Cu(Ac)_2$, the peaks at 1410 cm^{-1} (C=N stretching vibration), 1273 cm^{-1} (C–N stretching vibration), 1187 cm^{-1} (N–H in-plane deformation mode), and 1085 cm^{-1} (C–H in-plane deformation mode) are all split into duplex peaks, which indicates the existence of the ordered structures (Rastogi et al. 1997).

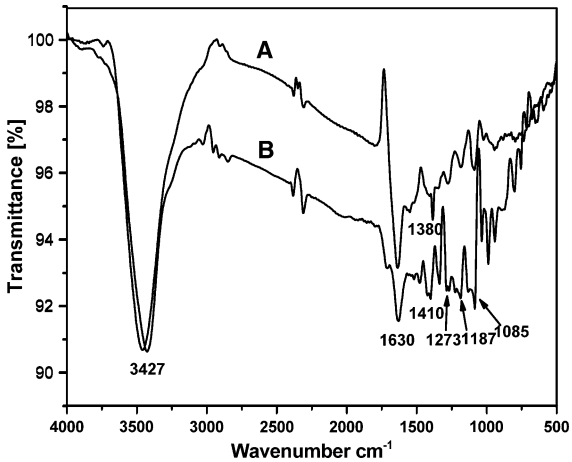

Fig. 6 FT-IR spectra of Ag/PPy NCs oxidized by (*A*) $AgNO_3$; (*B*) $Cu(Ac)_2$

The PPy sheath of Ag/PPy NCs–$Cu(Ac)_2$ was synthesized through oxidative polymerization of pyrrole during which Cu^{2+} ions were reduced to Cu^{+} ions accompanied with the redox polymerization of pyrrole monomers. The binding energy of N(1s), $Cu(2p_{3/2})$,C(1s), and Ag(3d) of NCs characterized by XPS are shown in Figs. 7 and 8, respectively. The binding energy of N(1s) electron for NCs–$Cu(Ac)_2$ in Fig. 7A has a 1.2-eV shift to the direction toward the higher binding energy compared with that for NCs–$AgNO_3$. The shift on binding energy of N(1s) can be illustrated by the increase on the electron density on imino group. Correspondingly the binding energy of $Cu(2p_{3/2})$ shown in Fig. 7(inset) also has a 0.9-eV

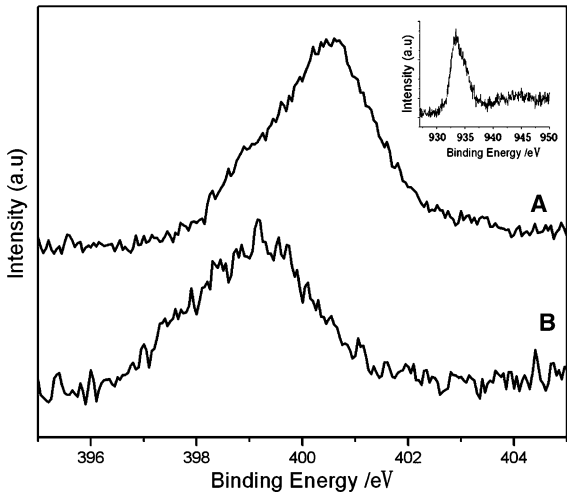

Fig. 7 XPS spectra for N(1s) of Ag/PPy NCs oxidized by (*A*) $Cu(Ac)_2$; (*B*) $AgNO_3$. *Inset* XPS spectrum for $Cu(2p_{3/2})$

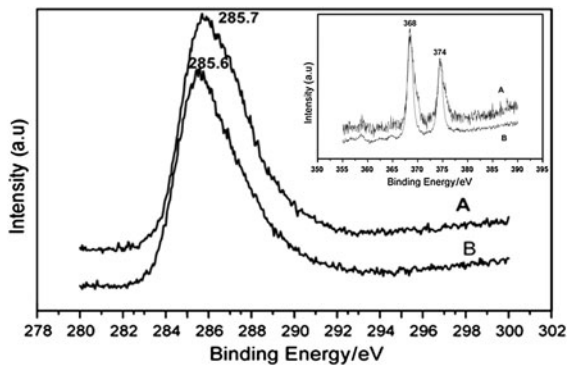

Fig. 8 XPS spectra for C(1s) of Ag/PPy NCs oxidized by (*A*) $AgNO_3$, (*B*) $Cu(Ac)_2$. *Inset* XPS spectrum for Ag(3d) (*A* $AgNO_3$, *B* $Cu(Ac)_2$)

shift with respect to the standard electron binding energy. The shifts on both N(1s) and Cu(2p3/2) peak in XPS spectra indicate the formation of strong Cu(I)–N bond. Although both C and N atoms on the pyrrole ring can contribute delocalized π electrons, N–Cu(I) bonds are more preferable to be formed rather than ring–Cu(I) bonds (Gao et al. 2004). The binding energies of C(1s) and Ag(3d) in Fig. 8 and inset do not show significant difference with the application of different oxidants. In this way, the strong Cu(I)–N bonds are identified in the sheath of Ag/PPy NCs–$Cu(Ac)_2$.

Conclusion

Through the redox polymerization of pyrrole monomers oxidized by Cu^{2+} ions adsorbed on the surface of silver NWs, Ag/PPy NCs were prepared at room temperature in aqueous solution. The thickness of polymer sheath was fairly depended on the concentration of Cu^{2+} adsorbed on the surface of silver NWs. Comparing the characterization results of SERS applied on Ag/PPy NCs using $Cu(Ac)_2$ and $AgNO_3$ as the oxidants, respectively, a special interfacial layer is detected with the pyrrole rings on PPy chains taking the identical conformation "standing" on the surface of Ag NWs when $Cu(Ac)_2$ were served as the oxidant. The existence of the interfacial structure was further proved by HR-TEM image of NCs–$Cu(Ac)_2$. FT-IR and XPS were also used to compare the structure difference on the PPy sheath synthesized using different oxidants. Although the main part of the polymer sheath was composed by PPy which was confirmed by FT-IR whatever oxidant was used, the sheath of the NCs oxidized by $Cu^{2+}(Cu(Ac)_2)$ is typical of Cu(I)–pyrrole coordinate structures with strong Cu(I)–N bond shown in XPS characterization.

Acknowledgments Financial support from NSFC (50673008) is gratefully acknowledged.

References

Chen F, Zhang J, Wang F, Shi G (2003) Raman spectroscopic studies on the structural changes of electrosynthesized polypyrrole films during heating and cooling processes. J Appl Polym Sci 89:3390–3395

Chen A, Kamata K, Nakagawa M, Iyoda T, Haiqiao W, Li X (2005) Formation process of silver-polypyrrole coaxial nanocables synthesized by redox reaction between AgNO3 and pyrrole in the presence of poly(vinylpyrrolidone). J Phys Chem B 109(39):18283–18288

Chen A, Xie H, Wang H, Li H, Li X (2006) Fabrication of Ag/polypyrrole coaxial nanocables through common ions adsorption effect. Synth Met 156:346

Davidson RG, Hammond LC, Turner TG, Wilson AR (1996) An electron and X-ray diffraction study of conducting polypyrrole/dodecyl sulfate. Synth Met 1996(81):1–7

Gao Y, Jiang P, Liu DF, Yuan HJ, Yan XQ, Zhou ZP, Wang JX, Song L, Liu LF, Zhou WY, Wang G, Wang CY, Xie SS, Zhang JM, Shen DY (2004) Evidence for the monolayer assembly of poly(vinylpyrrolidone) on the surfaces of silver nanowires. J Phys Chem B 108:12877–12881

Goldberger J, Hochbaum AI, Fan R et al (2006) Silicon vertically integrated nanowire field effect transistors. Nano Lett 6(5):973–977

Guo S, Li J, Ren W, Wen D, Dong S, Wang E (2009) Carbon nanotube/silica coaxial nanocable as a three-dimensional support for loading diverse ultra-high-density metal nanostructures: facile preparation and use as enhanced materials for electrochemical devices and SERS. Chem Mater 21(11):2247–2257

Han G, Yuan J, Shi G, Wei F (2005) Electrodeposition of polypyrrole/multiwalled carbon nanotube composite films. Thin Solid Films 474:64–69

Jang J, Bae J (2007) Carbon nanofiber/polypyrrole nanocable as toxic gas sensor. Sens Actuator B 122(1):7–13

Kiani MS, Bhat NV, Davis FJ, Mitchell GR (1992) Highly anisotropic electrically conducting films based on polypyrrole. Polymer 33:4113–4120

Kuemmeth F, Ilani S, Ralph DC, McEuen L (2008) Coupling of spin and orbital motion of electrons in carbon nanotubes. Nature 452:448–452

Mayya KS, Gittins DI, Dibaj AM, Caruso F (2001) Nanotubes prepared by templating sacrificial nickel nanorods. Nano Lett 1:727–730

Moskovits M, Suh JS (1984) Surface selection rules for surface-enhanced Raman spectroscopy: calculations and application to the surface-enhanced Raman spectrum of phthalazine on silver. J Phys Chem 88(23):5526–5530

Park S, Kim S, Han S (2007) Growth of homoepitaxial ZnO film on ZnO nanorods and light emitting diode applications. Nanotechnology 18:1–6

Rastogi S, Speolstra AB, Goossens JGP, Lemstra PJ (1997) Chain mobility in polymer systems: on the borderline between solid and melt. 1. Lamellar doubling during annealing of polyethylene. Macromolecules 30:7880–7889

Sun Y, Xia Y (2002) Large-scale synthesis of uniform silver nanowires through a soft, self-seeding, polyol process. Adv Mater 14:833–837

Tang Z, Kotov NA (2005) One-dimensional assemblies of nanoparticles: preparation, properties and promise. Adv Mater 17(8):951–962

Tian B, Zheng X, Kempa TJ, Fang Y, Yu N, Yu G, Huang J, Lieber CM (2007) Coaxial silicon nanowires as solar cells and nanoelectronic power sources. Nature 449:885–889

Wang W, Zhang R (2009) Silver–polypyrrole composites: facile preparation and application in surface-enhanced Raman spectroscopy. Synth Met 159:1332–1335

Wang W, Shi G, Zhang R (2009) Facile fabrication of silver/polypyrrole composites by the modified silver mirror reaction. J Mater Sci 44(11):3002–3005

Xia Y, Yang P, Sun Y, Wu Y, Mayers B, Gates B, Yin Y, Kim F, Yan H (2003) One-dimensional nanostructures: synthesis, characterization, and applications. Adv Mater 15(5):353–389

Xie H, Qiu T, Li Y (2008) Fabrication of Ag/polypyrrole (PPy) coaxial nanocables through ions adsorption method. Chem J Chin University 29(1):1046–1049

Xiong Y, Washio I, Chen J, Cai H, Li ZY, Xia Y (2006) Poly(vinyl pyrrolidone): a dual functional reductant and stabilizer for the facile synthesis of noble metal nanoplates in aqueous solutions. Langmuir 22:8563–8570

Xu J, Li X, Liu J, Wang X, Peng Q, Li Y (2005) Solution route to inorganic nanobelt-conducting organic polymer core–shell nanocomposites. J Polym Sci A 43:2892–2900

Yu S, Cui X, Li L et al (2004) From starch to metal/carbon hybrid nanostructures: hydrothermal metal-catalyzed carbonization. Adv Mater 16:1636–1640

Zhang X, Manohar SK (2005) Narrow pore-diameter polypyrrole nanotubes. J Am Chem Soc 127:14156–14157

Zhang Y, Suenaga K, Colliex C, Iijima S (1998) Coaxial nanocable: silicon carbide and silicon oxide sheathed with boron nitride and carbon. Science 281:973–975

Zhang W, Wen X, Yang S (2003) Synthesis and characterization of uniform arrays of copper sulfide nanorods coated with nanolayers of polypyrrole. Langmuir 19:4420–4426

Zhang Y, Wang L, Mascarenhas A (2007) Quantum coaxial cables for solar energy harvesting. Nano Lett 7(5):1264–1269